



## **Modeling and Control of PV-WIND Hybrid Microgrid in Grid Connected and Isolated Modes**

**P J Mohana Rao**

PG student

Dept. Electrical and Electronics Engineering  
Bapatla engineering college  
Bapatla, India.

**M Durga Prasada Rao**

Asst. professor

Dept. Electrical and Electronics Engineering  
Bapatla engineering college  
Bapatla, India.

### **ABSTRACT**

*Microgrid concept acts as a solution to integrate large amounts of micro sources without disrupting the operation of main utility grid. In this paper a hybrid microgrid is proposed in order to reduce the multiple conversions in an individual ac/dc microgrid. This hybrid microgrid consists of PV-WIND energy sources for DC and AC networks respectively. Energy storage systems can be connected to either AC or DC micro grids. The proposed hybrid microgrid can operated in grid-tied or isolated mode. AC sources and loads are connected to AC network, whereas DC sources and loads are connected to DC network. The coordination control schemes are proposed for smooth power exchange between AC and DC links under various supply and demand conditions. Uncertainty and intermittent characteristics of wind speed, solar irradiation level, ambient temperature and load also considered in system control and operation. This paper presents a small hybrid microgrid modeled and simulated using the Simulink in the MATLAB.*

**Index Terms**— Coordination control operation, Energy management, grid connected mode, grid operation, Hybrid microgrid, isolated mode, , PV system, Wind power generation.

### **Introduction**

Distribution generation (DG) technologies can provide energy solutions to customer's problems regarding reliability, high power quality issues. DG are having wide variety of alternatives with renewable or nonconventional energy resources are available, i.e., photovoltaic arrays, micro turbines, fuel cells, wind

turbines. These resources are connected to the utility through power electronic interfacing converters like inverter. DG is a suitable for high reliable electrical power supply, as it is capable to operate either in the islanded mode or in the grid-tied mode.

Recently renewable energy sources are attractive options for providing power in places where a connection to the utility network is either impossible or unduly expensive. As electric distribution technology steps into next century, many trends are becoming noticeable that will change the requirements of energy deliver. The ever increasing energy consumption, soaring cost and exhaustible nature of fossil fuels, and the worsening global environment have created increased interest in green power generation systems. Renewable sources have gained worldwide attention due to fast depletion of fossil fuels along with growing energy demand. On other hand, more and more dc loads such as light-emitting diode (LED) lights and electric vehicles are connected to ac power systems to save energy and reduce CO<sub>2</sub> emission. Long distance high voltage transmission is not necessary when power is fully supplied by local renewable power sources [1]. The concept of the microgrid has been evolved for smooth integration and control of distributed generations with the utility grid. AC microgrids [2]-[5] have been proposed to facilitate the connection of renewable power sources to conventional AC systems.

DC power from photovoltaic panels (PV) or fuel cells has to be converted into ac using dc/dc boosters and dc/ac inverters in order to connect to an ac grid. Recently, DC micro grids are resurging due to the

development and deployment of renewable dc power sources and their inherent advantage for dc loads in commercial, industrial and residential applications. The DC microgrid has been proposed to incorporate various distributed generators and ac sources have to be converted into dc before connected to a dc grid and dc/ac inverters are required for conventional ac loads [6]-[10]. DC microgrid cannot completely eliminate losses occurring in multiple stage conversions, though losses occurring in dc/dc conversions are lesser than those occurring in dc/ac or ac/dc conversions. Multiple reverse conversions are required in an individual ac or dc grids may add additional loss to the system operation and will make current home and office appliances more complicated. Thus, a hybrid microgrid is more beneficial to reduce the processes of multiple reverse conversions in an individual ac or dc micro grid to facilitate the connection of variable renewable ac and dc sources and loads with the power system in order to minimize the conversion losses. Since the operational issues of hybrid grid is more complicated than those of an individual ac and dc micro grids. A microgrid comprises of low voltage distributed systems with distributed generations, storage devices, loads and interconnecting switches. The operation of microgrids provide advantages of higher flexibility, better power quality, controllability, efficiency of operation, and bidirectional power flow between the utility grid and the microgrid in the grid connected mode of operation. This paper presents an analysis and performance of hybrid grid and various issues such as operating modes, coordination control algorithms among various converters to harness maximum power and stable operation of both ac and dc grids. Operating modes of microgrid are discussed. The advanced power electronics and control technologies used in this paper will make a future power grid much smarter.

## CONFIGURATION OF HYBRID MICROGRID

### A. Grid Configuration:

Fig.1 shows a conceptual hybrid system configuration where various ac and dc sources and loads are connected to the corresponding dc and ac networks.

The ac and dc links are connected together through two transformers and two four-quadrant operating three phase converters. The bus of the hybrid grid is tied to the utility grid.

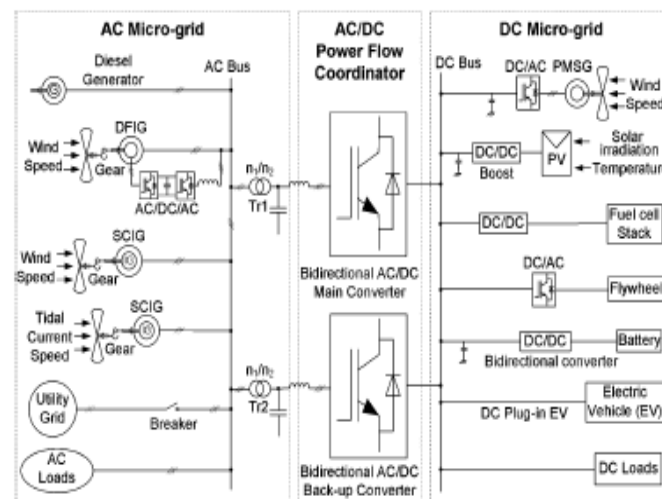


Fig. 1. A hybrid ac/dc microgrid system

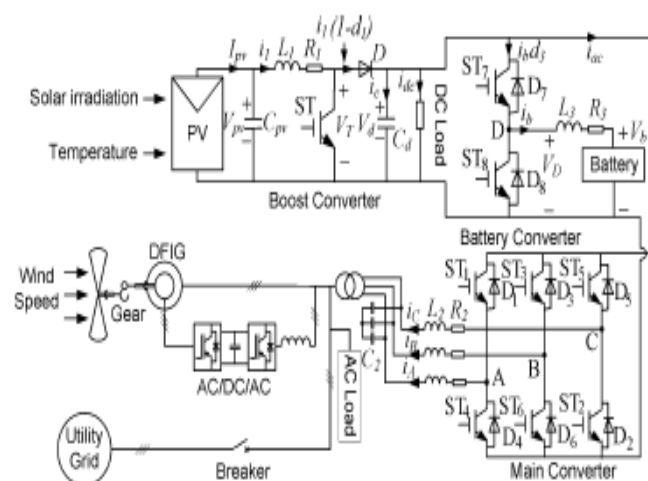


Fig.2. Representation of proposed hybrid grid.

In the proposed system, PV arrays are connected to dc bus through boost converter to simulate dc sources. A DFIG wind generation system is connected to ac bus to simulate ac sources. A battery with bidirectional dc/dc converter is connected to dc bus as energy storage. A variable dc and ac load are connected to their dc and ac buses to simulate various loads. PV modules are connected in series and parallel. As solar radiation level and ambient temperature changes the output power of solar panel alters. A capacitor Cpv is added

to PV terminal in order to suppress high frequency ripples of the PV output voltage. The converters share a common dc bus. A wind generation system consists of doubly fed induction generator with back to back AC/DC/AC PWM converter connected between the rotor through slip rings and ac bus. The ac and dc buses are coupled through a transformer and a main bidirectional power flow converter to exchange power between dc and ac sides. A hybrid microgrid can be operated in two modes, one is grid connected mode and other is isolated mode.

### B. Grid Operation:

The hybrid grid can operate in two modes. In grid-tied mode, the main converter is to provide stable dc bus voltage and required reactive power and to exchange power between the ac and dc buses. The boost converter and WTG are controlled to provide the maximum power. When the output power of the dc sources is greater than the dc loads, the converter acts as an inverter and injects power from dc to ac side. When the total power generation is less than the total load at the dc side, the converter injects power from the ac to dc side. When the total power generation is greater than the total load in the hybrid grid, it will inject power to the utility grid. Otherwise, the hybrid grid will receive power from the utility grid. In the grid tied mode, the battery converter is not very important in system operation because power is balanced by the utility grid. In autonomous mode, the battery plays a very important role for both power balance and voltage stability. Control objectives for various converters are dispatched by energy management system. DC bus voltage is maintained stable by a battery converter or boost converter according to different operating conditions. The main converter is controlled to provide a stable and high quality ac bus voltage. Both PV and WTG can operate on maximum power point tracking (MPPT) or off-MPPT mode based on system operating requirements. Variable wind speed and solar irradiation are applied to the WTG and PV arrays respectively to simulate variation of power of ac and dc sources and test the MPPT control algorithm.

### C. Modeling of PV Panel:

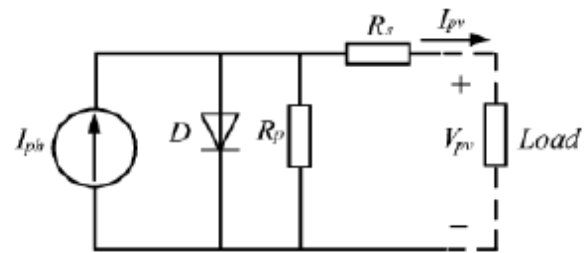


Fig.3 Equivalent ckt of solar cell.

Fig. 3 shows the equivalent circuit of a PV panel with a load. The current output of the PV panel is modeled by the following three equations [11], [12].

$$I_{pv} = n_p I_{ph} - n_p I_{sat} \times \left[ \exp \left( \left( \frac{q}{AkT} \right) \left( \frac{V_{pv}}{n_s} + I_{pv} R_s \right) \right) - 1 \right] \quad (1)$$

$$I_{ph} = (I_{ss0} + k_i(T - T_r)) \cdot \frac{S}{1000} \quad (2)$$

$$I_{sat} = I_{rr} \left( \frac{T}{T_r} \right)^3 \exp \left( \left( \frac{qE_{gap}}{kA} \right) \cdot \left( \frac{1}{T_r} - \frac{1}{T} \right) \right) \quad (3)$$

### D. Modeling of Battery

Battery acts as a constant voltage load line on PV array and is charged both by PV array and induction generator. The battery is modeled as a nonlinear voltage source whose output voltage depends not only on the current but also on the battery state of charge (SOC), which is non linear function of the current and time

$$V_b = V_0 + R_b \cdot i_b - K \frac{Q}{Q + \int i_b dt} + A \cdot \exp(B \int i_b dt) \quad (4)$$

$$SOC = 100 \left( 1 + \int \frac{i_b}{Q} dt \right) \quad (5)$$

### E. Modeling of Wind Turbine Generator:

The power output of wind turbine generator (WTG) is determined by

$$P_m \approx 0.5 \rho A C_p(\lambda, \beta) V_\omega^3 \quad (6)$$

Where  $\rho$  is air density,  $A$  is rotor swept area,  $V_\omega$  is wind speed, and  $C_p(\lambda, \beta)$  is the power coefficient, which is the function of tip speed ratio  $\lambda$  and  $\beta$  is pitch angle.

## COORDINATION CONTROL OF THE CONVERTERS

There are five types of converters in the hybrid grid. Those converters have to be coordinately controlled with the utility grid to supply an uninterrupted, high efficiency, and high quality power to variable dc and ac loads under variable solar irradiation and wind speed when the hybrid grid operates in both isolated and grid tied modes. The control algorithms for those converters are presented in this section. When the hybrid grid operates in grid connected mode, the control objective of the boost converter is to track the MPPT of the PV array by regulating its terminal voltage. The back-to-back ac/dc/ac converter of the DFIG is controlled to regulate rotor side current to achieve MPPT and to synchronize with ac grid.

$$P_{pv} + P_{ac} = P_{dcL} + P_b \quad (7)$$

$$P_s = P_w - P_{acL} - P_{ac} \quad (8)$$

In isolated mode, the battery converter operates either in charging or discharging mode based on power balance in the system. The dc-link voltage is maintained by either battery or boost converter based on system operating conditions. Power under various load and supply conditions should be balanced as follows:

$$P_{pv} + P_w = P_{acL} + P_{dcL} + P_{loss} + P_b \quad (9)$$

Where  $P_{loss}$  is the total grid loss.

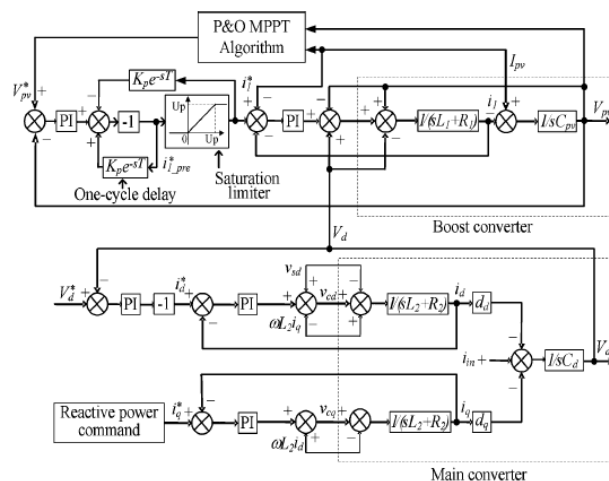


Fig. 4. The control block diagram for boost converter and main converter in grid connected mode.

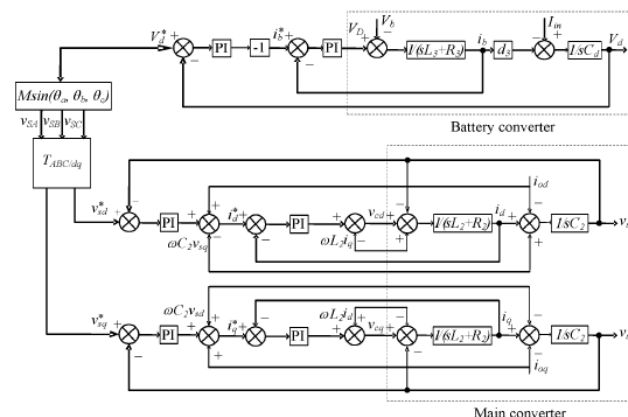


Fig. 5. Block diagram of the battery and main converters for the normal case in isolated mode.

## SIMULATION RESULTS

The operations of the hybrid grid under various source and load conditions are simulated to verify the proposed control algorithms. The parameters of components for the hybrid grid are listed in Table I

### A. Grid-Connected Mode

In this mode, the main converter operates in the PQ mode. Power is balanced by the utility grid. The battery is fully charged and operates in the rest mode in the simulation. AC bus voltage is maintained by the utility grid and dc bus voltage is maintained by the main converter.



The optimal terminal voltage is determined using the basic P&O algorithm based on the corresponding solar irradiation. The voltages for different solar irradiations are shown in Fig. 9. The solar irradiation level is set as 400 W/m<sup>2</sup> from 0.0 s to 0.1 s, increases linearly to 1000 W/m<sup>2</sup> from 0.1 s to 0.2 s, keeps con-stant until 0.3 s, decreases to 400 W/m<sup>2</sup> from 0.3 s to 0.4 s and keeps that value until the final time 0.5 s. The initial voltage for the P&O is set at 250 V. It can be seen that the P&O is continu-ously tracing the optimal voltage from 0 to 0.2 s. The algorithm only finds the optimal voltage at 0.2 s due to the slow tracing speed. The algorithm is searching the new optimal voltage from 0.3 s and finds the optimal voltage at 0.48 s. It can be seen that the basic algorithm can correctly follow the change of solar irra-diation but needs some time to search the optimal voltage. The improved P&O methods with fast tracing speed should be used in the PV sites with fast variation of solar irradiation.

Fig. 9 shows the curves of the solar radiation (radiation level times 30 for comparison) and the output power of the PV panel. The output power varies from 13.5 kW to 37.5 kW, which closely follows the solar irradiation when the ambient temperature is fixed.

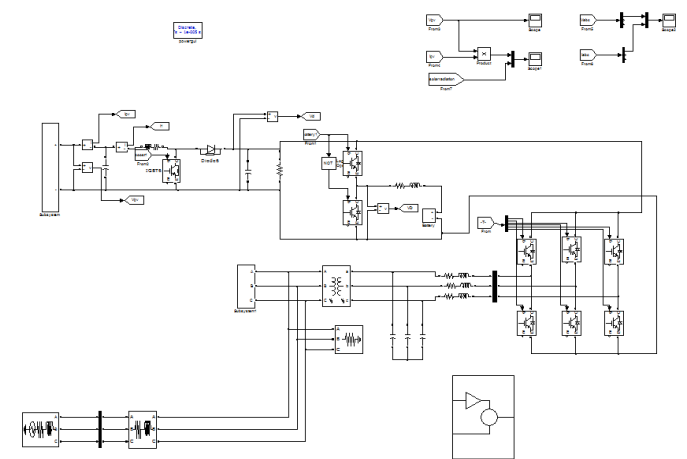
The voltage (voltage times 0.2 for comparison) and current responses at the ac side of the main converter when the solar irradiation level decreases from 1000 W/m<sup>2</sup> at 0.3 s to 400 W/m<sup>2</sup> at 0.4 s with a fixed dc load 20 kW. It can be seen from the current directions that the power is injected from the dc to the ac grid before 0.3 s and reversed after 0.4 s

The voltage (voltage times 0.2 for comparison) and current responses at the ac side of the main converter when the dc load increases from 20 kW to 40 kW at 0.25 s with a fixed irradiation level 750 W/m<sup>2</sup> . It can be seen from the current direction that power is injected from dc to ac grid before 0.25 s and reversed after 0.25 s. The voltage response at dc side of the main converter under the same conditions. The figure shows that the voltage drops at 0.25 s and recovers quickly by

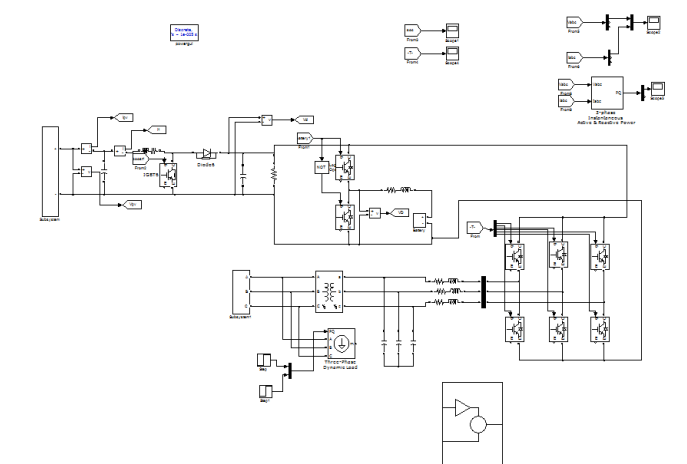
the controller.

TABLE III  
COMPONENT PARAMETERS FOR THE HYBRID GRID.

Symbol	Description	Value
$C_{pv}$	Capacitor across the solar panel	110uF
$L_1$	Inductor for the boost converter	2.5mH
$C_d$	Capacitor across the dc-link	4700uF
$L_2$	Filtering inductor for the inverter	0.43mH
$R_2$	Equivalent resistance of the inverter	0.3ohm
$C_2$	Filtering capacitor for the inverter	60uF
$L_3$	Inductor for the Battery converter	3mH
$R_3$	Resistance of L3	0.1ohm
$f$	Frequency of the AC grid	60Hz
$f_s$	Switching frequency of power converters	10kHz
$V_d$	Rated DC bus voltage	400V
$V_{il\_rms}$	Rated AC bus line voltage ( <i>rms value</i> )	400V
$n_1/n_2$	Ratio of the transformer	2:1



**Fig.6.Simulation circuit of hybrid microgrid in grid connected mode**



**Fig.7.simulink model of hybrid microgrid in isolated mode**

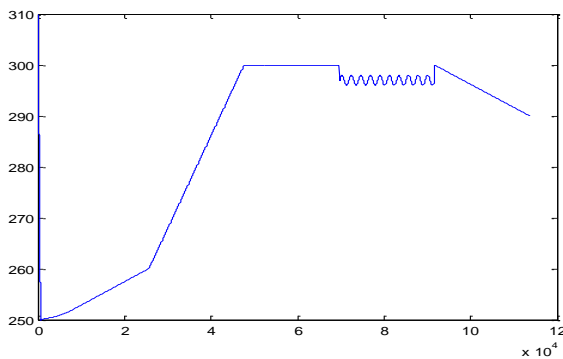


Fig. 8. The terminal voltage of the solar panel.

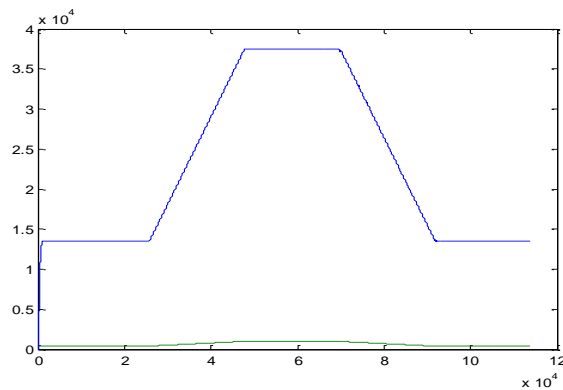


Fig. 9. PV output power versus solar irradiation.

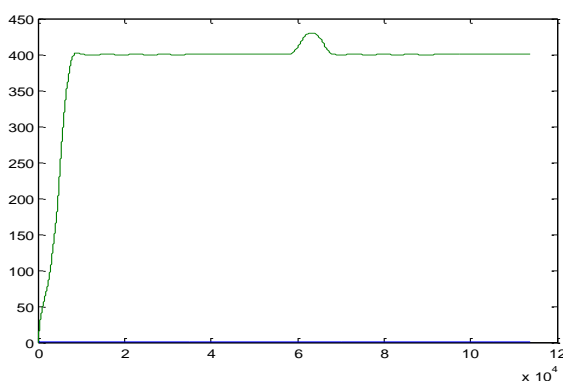


Fig. 10. DC bus voltage transient response.

dynamic responses at the ac side of the main

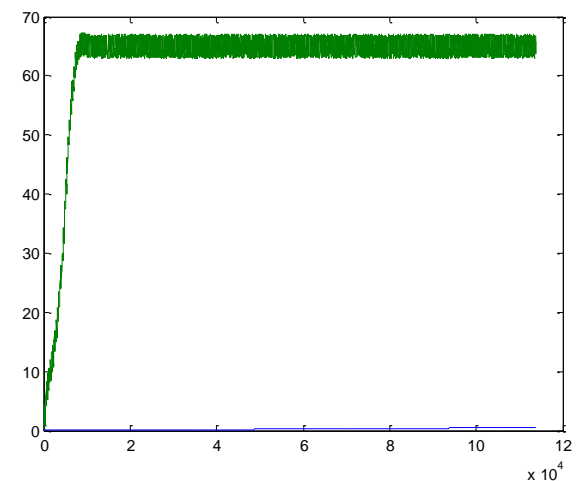
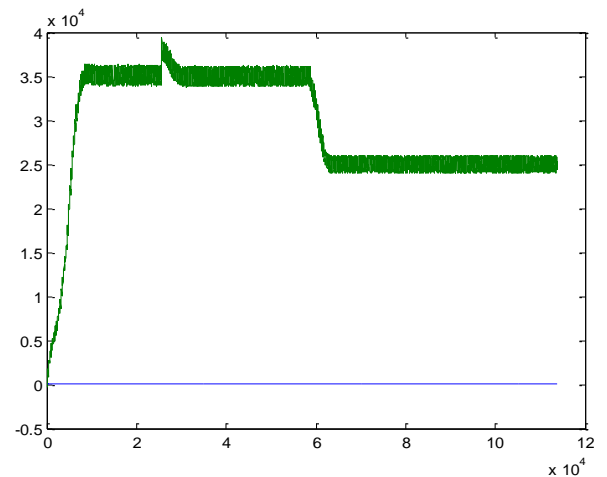
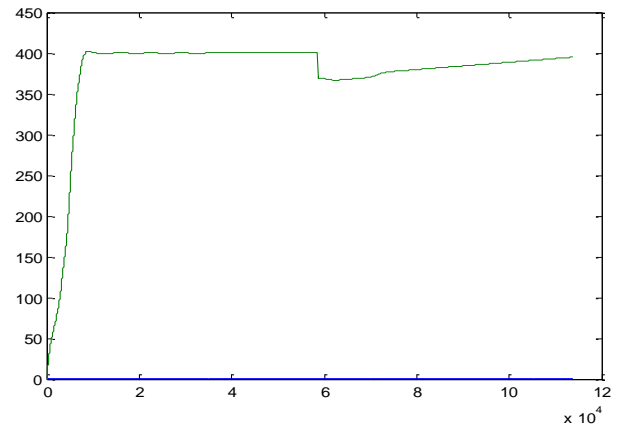


Fig. 11. DC bus voltage, PV output power, and battery current for isolated mode

### B. Isolated Mode:

The control strategies for the normal case and Case 1 are verified. In the normal case, dc bus voltage is maintained stable by the battery converter and ac bus voltage is provided by the main converter. The reference of dc-link voltage is set as 400V. The

converter when the ac load increases from 20 kW to 40 kW at 0.3 s with a fixed wind speed 12 m/s. It is shown clearly that the ac grid injects power to the dc

grid before 0.3 s and receives power from the dc grid after 0.3 s. The voltage at the ac bus is kept 326.5 V constant regardless of load conditions. The nominal voltage and rated capacity of the battery are selected as 200 V and 65 Ah respectively. The transient process of the DFIG power output, which becomes stable after 0.45 s due to the mechanical inertia.

Fig. 12 shows the current and SOC of the battery. The total power generated is greater than the total load before 0.3 s and less than the total load after 0.3 s. It can be seen from Fig. 12 that the battery operates in charging mode before 0.3 s because of the positive current and discharging mode after 0.3 s due to the negative current. The SOC increases and decreases before and after 0.3 s respectively.

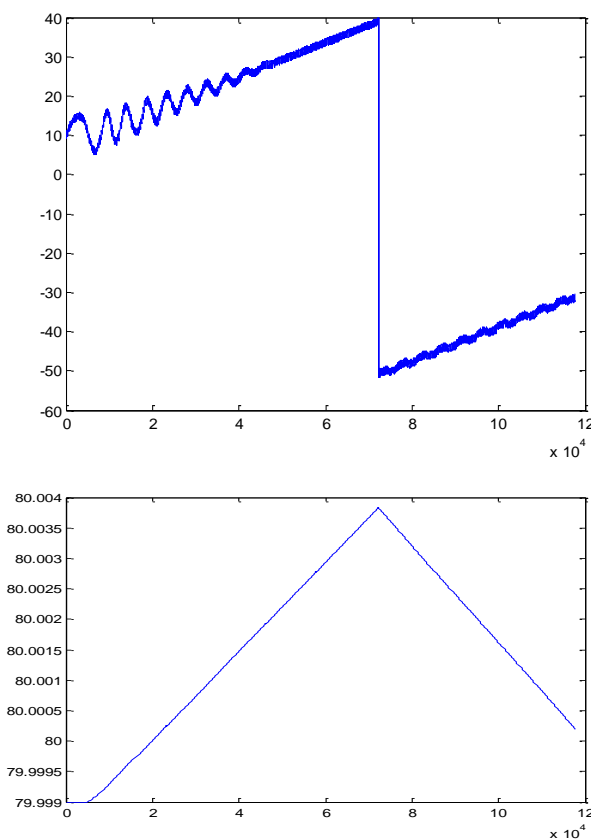


Fig. 12. Battery charging current (upper) and SOC (lower) for the normal case.

When the system is at off-MPPT mode in Case 1, the dc bus voltage is maintained stable by the boost converter and ac bus voltage is provided by the main converter. Fig. 11 shows the dc bus voltage, PV output power, and battery charging current respectively when the dc load decreases from 20 kW to 10 kW at 0.2 s with a constant solar irradiation level 1000 W/m<sup>2</sup>.

The battery discharging current is kept constant at 65 A. The dc bus voltage is stabilized to 400 V after 0.05 s from the load change. The PV power output drops from the maximum value after 0.2 s, which means that the operating modes are changed from MPPT to off-MPPT mode. The PV output power changes from 35 kW to 25 kW after 0.2 s.

## CONCLUSION

In this paper, the hybrid grid system configuration is done in MATLAB/SIMULINK environment. The process of multiple reverse conversions in an individual AC or DC grid can be reduced. The simulation results show that the hybrid grid can operate stably in the grid-tied or isolated mode. Here proposed controllers are developed for all converters to maintain stable system under various resource and load changing conditions. The total system efficiency depends on the reduction of conversion losses and increase for an extra dc link. It is also difficult for companies to redesign their home and office products without the embedded ac/dc rectifiers although it is theoretically possible. Therefore, the hybrid grids may be implemented when some small customers want to install their own PV systems on the roofs and are willing to use LED lighting systems and EV charging systems. The hybrid grid may also be feasible for some small isolated industrial plants with both PV system and wind turbine generator as the major power supply.

## REFERENCES

- [1] R. H. Lasseter, "MicroGrids," in *Proc. IEEE Power Eng. Soc. Winter Meet.*, Jan. 2002, vol. 1, pp. 305–308.

- [2] Y. Zoka, H. Sasaki, N. Yorino, K. Kawahara, and C. C. Liu, "An inter-action problem of distributed generators installed in a MicroGrid," in *Proc. IEEE Elect. Utility Deregulation, Restructuring. Power Technol.*, Apr. 2004, vol. 2, pp. 795–799
- [3] Y. Ito, Z. Yang, and H. Akagi, "DC micro-grid based distribution power generation system," in *Proc. IEEE Int. Power Electron. Motion Control Conf.*, Aug. 2004, vol. 3, pp. 1740–1745.
- [4] A. Sannino, G. Postiglione, and M. H. J. Bollen, "Feasibility of a DC network for commercial facilities," *IEEE Trans. Ind. Appl.*, vol. 39, no. 5, pp. 1409–1507, Sep. 2003.
- [5] D. J. Hammerstrom, "AC versus DC distribution systems-did we get it right?," in *Proc. IEEE Power Eng. Soc. Gen. Meet.*, Jun. 2007, pp. 1–5.
- [6] D. Salomonsson and A. Sannino, "Low-voltage DC distribution system for commercial power systems with sensitive electronic loads," *IEEE Trans. Power Del.*, vol. 22, no. 3, pp. 1620–1627, Jul. 2007..
- [7] O. Tremblay, L. A. Dessaint, and A. I. Dekkiche, "A generic battery model for the dynamic simulation of hybrid electric vehicles," in *Proc. IEEE Veh. Power Propulsion Conf. (VPPC 2007)*, pp. 284–289.
- [8] D. W. Zhi and L. Xu, "Direct power control of DFIG with constant switching frequency and improved transient performance," *IEEE Trans. Energy Conv.*, vol. 22, no. 1, pp. 110–118, Mar. 2007.
- [9] Bo and M. Shahidehpour, "Short-term scheduling of battery in a grid-connected PV/battery system," *IEEE Trans. Power Syst.*, vol. 20, no. 2, pp. 1053–1061, May 2005.
- [10] S. A. Daniel and N. AmmasaiGounden, "A novel hybrid isolated gener-ating system based on PV fed inverter-assisted wind-driven induction generators," *IEEE Trans. Energy Conv.*, vol. 19, no. 2, pp. 416–422, Jun. 2004.
- [11] D. Sera, R. Teodorescu, J. Hantschel, and M. Knoll, "Optimized max-imum power point tracker for fast-changing environmental conditions," *IEEE Trans. Ind. Electron.*, vol. 55, no. 7, pp. 2629–2637, Jul. 2008
- [12] .B. Bryant and M. K. Kazimierczuk, "Voltage loop of boost PWM DC-DC converters with peak current-mode control," *IEEE Trans. Circuits Syst. I, Reg. Papers*, vol. 53, no. 1, pp. 99–105, Jan. 2006.
- [13] S. Arnalte, J. C. Burgos, and J. L. Rodriguez-amenado, "Direct torque control of a doubly-fed induction generator for variable speed wind turbines," *Elect. Power Compon. Syst.*, vol. 30, no. 2, pp. 199–216, Feb. 2002.
- [14] W. S. Kim, S. T. Jou, K. B. Lee, and S. Watkins, "Direct power control of a doubly fed induction generator with a fixed switching frequency," in *Proc. IEEE Ind. Appl. Soc. Annu. Meet.*, Oct. 2008, pp. 1–9
- [15] .E. Koutroulis and K. Kalaitzakis, "Design of a maximum power tracking system for wind-energy-conversion applications," *IEEE Trans. Ind. Electron.*, vol. 53, no. 2, pp. 486–494, Apr. 2006.
- [16] D. J. Hammerstrom, "AC versus DC distribution systems-did we get it right?," in *Proc. IEEE Power Eng. Soc. Gen. Meet.*, Jun. 2007, pp. 1–5
- [17] .D. Salomonsson and A. Sannino, "Low-voltage DC distribution system for commercial power systems with sensitive electronic



loads,” *IEEE Trans. Power Del.*, vol. 22, no. 3, pp. 1620–1627, Jul. 2007.

- [18] M. E. Ropp and S. Gonzalez, “Development of a MATLAB/simulink model of a single-phase grid-connected photovoltaic system,” *IEEE Trans. Energy Conv.*, vol. 24, no. 1, pp. 195–202, Mar. 2009.
- [19] K. H. Chao, C. J. Li, and S. H. Ho, “Modeling and fault simulation of photovoltaic generation systems using circuit-based model,” in *Proc. IEEE Int. Conf. Sustainable Energy Technol.*, Nov. 2008, pp. 290–294
- [20] O. Tremblay, L. A. Dessaint, and A. I. Dekkiche, “A generic battery model for the dynamic simulation of hybrid electric vehicles,” in *Proc. IEEE Veh. Power Propulsion Conf. (VPPC 2007)*, pp. 284–289.

## Authors Details:



**P J Mohana rao.** born on 20<sup>th</sup> june 1989 at Mangalagiri. He received his B.Tech degree in the year 2010, In the stream of Electrical and Electronics Engineering, in narasaraopet engg college, narasaraopeta Guntur Dist, Andhra Pradesh. Pursuing M.Tech in the stream of power systems in Bapatla engineering college, Bapatla, Guntur Dist.



**Durga Prasada Rao.** M. born on 20th Feb 1981 at Velangi. He received his B.Tech, M.Tech degree in the year 2006, 2009 respectively in the stream of Power electronics and Power systems, EEE Department, in K.L University, Vaddeswaram, Guntur Dist, Andhra Pradesh. He has been working as a Asst. Professor from the past 5 years in the Bapatla engineering college, Bapatla Assitant Professor in EEE Department . His current interest is on improving the stability analysis, harmonic reduction using the FACT Devices.